Synthetic Metals 245 (2018) 32–41

Contents lists available at ScienceDirect

Synthetic Metals

journal homepage: www.elsevier.com/locate/synmet

Synergetic effect in a self-doping polyaniline/TiO_2 composite for selective adsorption of heavy metal ions

Jie Chen, Ning Wang, Yunpeng Liu, Jinwei Zhu, Jiangtao Feng*, Wei Yan*

Department of Environmental Science and Engineering, State Key Laboratory of Multiphase Flow in Power Engineering, Xi'an Jiaotong University, Xi'an 710049, PR China

ARTICLE INFO

Keywords:
PANi(ES^+)/TiO_2(O-) heterojunction structure
Heavy metal ions
Selective adsorption
Synergistic adsorption
Mechanism

ABSTRACT

Design and synthesis of adsorbents with high adsorption selectivity are important for the treatment of the wastewater which contains multiple metal ions. Herein, a PANi(ES^+)/$TiO_2(O^-)$ composite is the subject of an investigation into the synergetic effect of a polymer/metal oxide composite and the mechanism of selective adsorption towards heavy metal ions. The self-doping nature of $TiO_2(O^-)$ to PANi was first discovered through characterizations including FT-IR, zeta potential analysis, TGA, XRD, SEM-EDS, TEM-EDS, N_2 adsorption-desorption isotherm and isotherm investigation for Pb (II), Zn (II) and Cu (II) in single/multiple metal ion system, which was confirmed to contribute to the novel selectivity of the PANi/TiO_2 composite of $Zn^{2+} > Pb^{2+} > > Cu^{2+}$ in a multiple metal ion system. The synergistic mechanism between the conjugated polymer and metal oxide for selective adsorption was discussed and proposed subsequently, which was suggested that the metastability of the doped state of PANi (ES^+) would result in the dedoping of the $TiO_2(O^-)$ in a non-acid solution (pH = 5), further leading to the doping of cationic heavy metal ions on $TiO_2(O^-)$. The mechanism we proposed can satisfactorily explain the selective adsorption properties of the polymer/metal oxide composite system and provide general guidance for designing an adsorbent with expected selective adsorption properties for water treatment.

1. Introduction

Currently, large amounts of wastewater containing various heavy metal ions such as Pb(II), Zn(II), Cu(II), *etc.* are being released into natural water system, resulting in serious water contamination and threats to human health [1,2]. Therefore, the heavy metal ions in wastewater should be removed and recycled before the water is discharged into the environment. So far, the removal of heavy metal ions from wastewater can be achieved by employing various methods including chemical precipitation [3], ionic exchange [4], coagulation [5], membrane separation [6], adsorption [7], *etc*. Among them, adsorption is widely investigated and applied due to its simplicity, high selectivity, low cost and excellent efficiency [8–10]. To achieve high adsorption efficiency in wastewater that contains multiple metal ions, considerable attention needs to be paid to the design and synthesis of adsorbents with high adsorption selectivity and adsorption capacity. However, few investigations into materials with these properties have been carried out.

Electroactive polymers such as polyaniline (PANi), polypyrrole (PPy) and polythiophene (PTh) with intrinsic redox properties and interesting doping and dedoping capabilities have been identified as candidates for adsorbents [7,8,11]. The polymer, PANi has attracted considerable research interest in recent years as an adsorbent [11]. Aniline polymers have the general form of $[(\text{-B-NH-B-NH})_y(\text{-B-N=Q=N-})_{1-y}]_n$, in which Q and B represent the quinoid and benzenoid ring, respectively. Therefore, it can exist mainly in four forms shown in Scheme ***S1***: i) the fully oxidized form, pernigraniline (PNA, y = 0); ii) 75% oxidized form, nigraniline (NA, y = 0.25); iii) 50% oxidized form, emeraldine base (EB, y = 0.5); iv) fully reduced form, leucoemeraldine base (LB, y = 0) [12]. Among them, the emeraldine base is the most common form, and can be doped into the emeraldine salt (ES) conducting state. The stability of the ES can be tuned by the solution pH, by which the doping process can be well controlled [12]. The ES will retain the doping ions when dry, however it will undergo dedoping gradually when it is in water with a pH greater than 4 [12,13]. Therefore, PANi with this interesting property will be taken into consideration when a PANi adsorbent is being designed.

In order to obtain an adsorbent with sensitive selectivity, heterogenous materials can be introduced to synergistically assist the PANi to selectively adsorb heavy metal ions [14]. Metal oxides are widely

* Corresponding authors.
E-mail addresses: j.chen@stu.xjtu.edu.cn (J. Chen), wangning7605@stu.xjtu.edu.cn (N. Wang), liuyunpeng1994@stu.xjtu.edu.cn (Y. Liu), 517157908@qq.com (J. Zhu), fjtes@xjtu.edu.cn (J. Feng), yanwei@xjtu.edu.cn (W. Yan).

https://doi.org/10.1016/j.synthmet.2018.08.006
Received 10 June 2018; Received in revised form 1 August 2018; Accepted 10 August 2018

regarded as encouraging adsorbents in this respect [15]. It has been reported that Mn oxides show special adsorption affinity toward Cu(II) [16] and Fe oxides possess unique affinity to Pb(II) [17], while Zn(II) can be greatly attracted to Si oxides [18]. Therefore, the synthesis of conducting polymers with metal oxides has been extensively researched. V. Gilja et al. [19], X. Li et al. [20] and M. Vaez et al. [21] investigated the synergetic effect between PANi and TiO_2 in the photocatalytic degradation of dye. In the synergetic mechanism they provided in these investigation, PANi played an important role in protecting the TiO_2 surface from the blockage of intermediates while TiO_2 absorbs photons with energy higher than 3.2 eV to generate the excited states of electron and hole pairs to oxidize the dye into CO_2 and H_2O. In addition, several interesting selective adsorption properties were also noted in investigations of PANi based metal oxides. S.A. Nabi et al. [22] prepared a PANi/Ti(V) tungstate composite, and showed selective adsorption for Pb(II), Hg(II), Bi(III) and Zr(IV). The reason of the selectivity was ascribed to the radius of the ions. In contrast, special affinity to Cu(II) and Pb(II) was acquired for PANi/Al_2O_3 in investigation conducted by S. Piri et al. [23] when the ions have to compete with Zn (II), Ni(II), Co(II) and Cd(II). Moreover, Q. Zhang et al. [24,25] prepared PANi/ZrP with or without carbon nanotubes (CNTs), observing that PANi/zirconium phosphate (ZrP) with CNTs showed better affinity to Pb(II) due to complexation with oxygen derived from P-O-H on the ZrP, while the composite without CNTs obtained in acetonitrile exhibited an affinity to Ni(II) due to artificial amino acids on ZrP to Ni(II), even though Ni(II) has a smaller radius than usually expected for heavy metal ions with such high affinity. Therefore, it can be seen that there still are many contradictions to the conclusions made previously for the selective adsorption mechanism, and the theory proposed before cannot satisfactorily explain the selectivity of the polymer/metal oxide composite. These contradictions can seriously restrict adsorbent design. While the combination of polymer and metal oxides produce the selective adsorption for heavy metal ions, the mechanism for the synergetic effect remains unknown. Therefore, a reasonable and convincing mechanism for the selective adsorption and the synergistic adsorption should be investigated and proposed.

To solve this problem, a PANi capable of doping and dedoping was chosen to synergistically combine with $TiO_2(O^-)$ in this study. The doping states, composite structure, textural properties and interaction of/between PANi and $TiO_2(O^-)$ were characterized using FT-IR, zeta potential analysis, TGA, XRD and N_2 adsorption-desorption isotherm. Adsorption experiments including kinetic, isotherm in single/multiple metal ion system were designed and performed to illuminate the individual and competitive adsorption properties for Pb(II), Zn(II) and Cu (II). Finally, a hypothesis for the synergistic mechanism between the polymer and $TiO_2(O^-)$ and the selective adsorption mechanism of polymer/$TiO_2(O^-)$ for heavy metal ions were verified by the results. The mechanism we proposed may provide insight to the nature of adsorption and may guide the design of adsorbents with selectivity towards certain heavy metal ions.

2. Experimental

2.1. Chemicals

The chemicals (AR grade) used in this investigation were all purchased from Sinopharm Chemical Reagent Co., Ltd (China). Specifically, aniline was purified by distillation, and stored in the refrigerator in the dark. The heavy metal ion solutions employed in the adsorption investigations were prepared from $Pb(NO_3)_2$, $Cu(NO_3)_2{\cdot}3H_2O$ and $Zn(NO_3)_2{\cdot}6H_2O$, respectively with ultrapure water.

2.2. Synthesis of the PANi(ES), TiO_2(OH) and PANi(ES^+)/$TiO_2(O^-$) composite

The PANi(ES^+)/$TiO_2(O^-$) composite was synthesized by chemical oxidative polymerization. The ratio of TiO_2 and aniline monomer was optimised in our previous work [26]. Specifically, the TiO_2 was prepared through the typical sol-gel hydrolysis. 20 mL of titanium (IV) isopropoxide (0.033 mol) was added in the aqueous solution (2.64 g). The obtained TiO_2 was then dispersed in 100 mL (0.1 mol·L^{-1}) of HNO_3 solution (Caution! HNO_3 is highly corrosive!), followed by adding 1.8 mL of aniline to the TiO_2 suspension (Caution! Aniline may cause cancer!). After stirring for 30 min, 22.8 g of ammonium persulphate (0.1 mol) was dispersed in the solution and was left for reaction to another 6 h at ambient temperature (Caution! Ammonium persulphate is corrosive!). The composite was filtrated and dried at 50 °C. The PANi (ES) and TiO_2(OH) used for comparison in this investigation were also synthesized using the same procedure, either without TiO_2 or aniline and ammonium persulphate being added.

2.3. Characterization

The Fourier transform infrared spectra (FT-IR) of the PANi(ES), TiO_2(OH) and PANi(ES^+)/$TiO_2(O^-$) composite used for the functional group characterization before and after metal ions adsorption were performed on a BRUKER TENSOR 37 FT-IR spectrometer by the KBr pellet method in the experimental range from 4000 to 400 cm^{-1}. The zeta potential investigation for the doping degree study was conducted on a Malvern Zetasizer Nano ZS90. The thermogravimetric analysis (TGA) used for the thermal stability study and the component inspection was performed on a Setaram Labsys Evo in N_2 flow with a heating rate of 10 °C min^{-1}. X-ray diffraction (XRD) patterns were acquired on an X'Pert PRO Diffractometer using a Cu-Kα radiation method. The N_2 adsorption and desorption isotherms were recorded on a Builder SSA-4200. The features including specific surface area, total pore volume and average pore radius were calculated using a Builder analysis software. A Shimadzu UV2600 spectrophotometer was applied for the solid UV–vis NIR spectra investigation on the PANi(ES^+)/$TiO_2(O^-$) composite synthesized through the Buchwald-Hartwig reaction. The scanning electron microscopy (SEM) and energy dispersive spectrometer (SEM-EDS) images were recorded on a JSM-6700 F to investigate the morphology of sample. A JEM model 2100 electron microscope was used to acquire the transmission electron microscopy (TEM) and energy dispersive spectrometer (TEM-EDS) images. The initial and residual concentrations of the heavy metal ions were determined on an inductive coupled plasma emission spectrometer (ICPE-9000, Shimadzu).

2.4. Adsorption experiments

In the adsorption experiments, the dose of adsorbent was kept at the optimal concentration of 2 g·L^{-1} with the solution volume of 20 mL. All experiments were performed using a benchtop shaking incubator (ZWY-100H, Zhicheng, Shanghai, China) with controllable temperature, and the agitation speed was kept at 200 rpm. The initial solution pH, which was determined using a TISAB (PXSJ-216F, Leici, Shanghai, China) by calibration in every test, was kept at 5 to avoid the influence of precipitation of heavy metal ions on the adsorption.

To study the isotherm in the single metal ion solution, Pb^{2+}, Zn^{2+} and Cu^{2+} solutions with various initial concentrations were applied at 15, 25, 45 °C, respectively for 3 h. The initial concentrations of Pb^{2+} were 100, 200, 300, 400, 600, 800 mg·L^{-1}, respectively, while the initial concentrations of Zn^{2+} and Cu^{2+} were 10, 50, 100, 200, 400, 600 mg·L^{-1}, respectively. To investigate the selectivity of the composite, a Pb^{2+}, Zn^{2+} and Cu^{2+} mixed solution with initial concentrations of 50, 100, 200, 300 and 400 mg·L^{-1} of each metal ion were used at 25 °C for 3 h. To study the effect of pH, solutions with initial pHs from 1 to 5 were employed for 3 h, and the initial heavy metal ion concentration was kept at 200 mg·L^{-1}. The initial pH was adjusted using dilute HNO_3 and NaOH solutions.

The adsorption capacity in the adsorption experiments and the recycling efficiency in the recycling experiments were calculated as

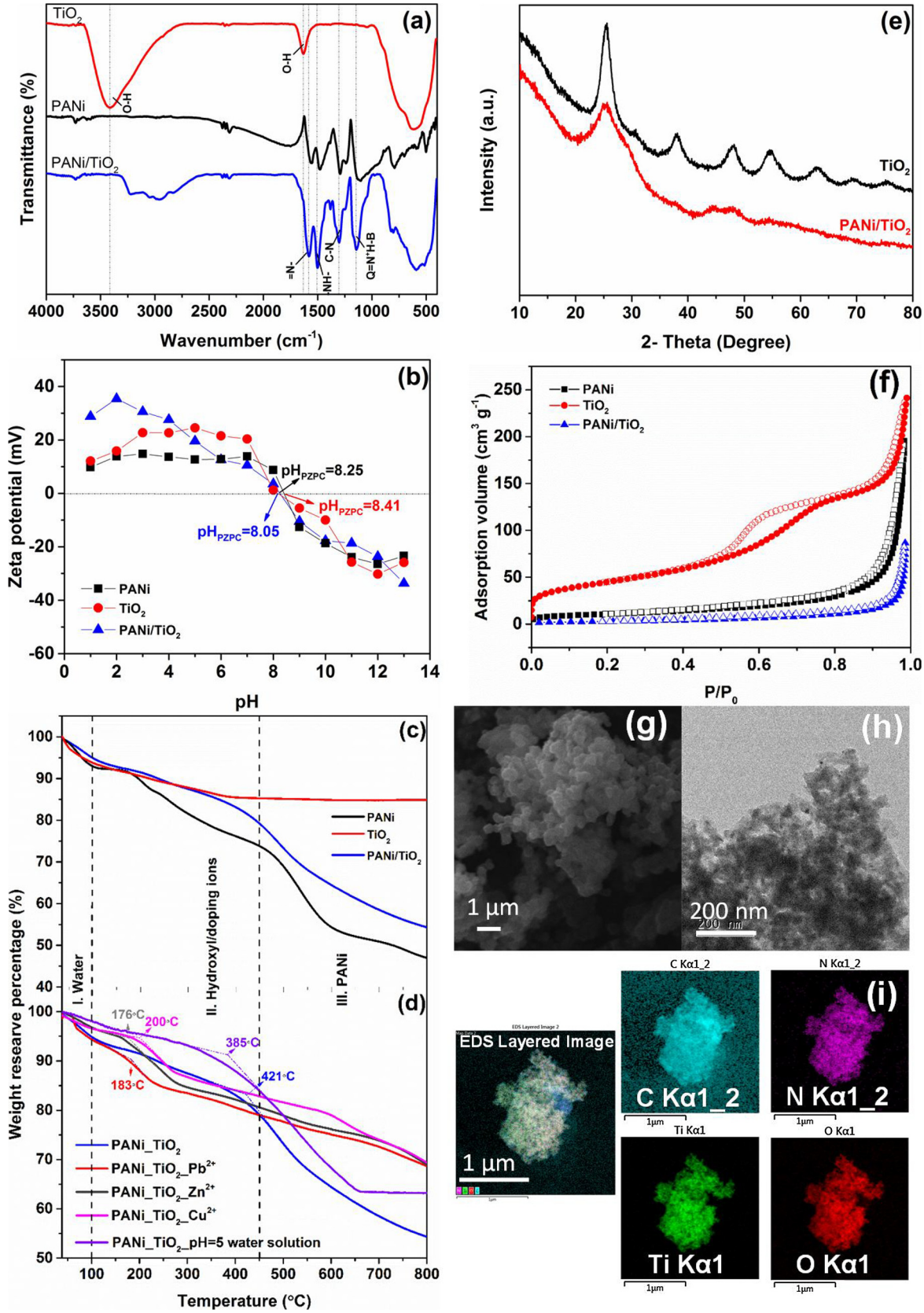

Fig. 1. Characterization of the PANi/TiO_2 composite: (a) FT-IR spectra of PANi(ES), TiO_2 and the PANi(ES^+)/TiO_2(O^-) composite; (b) Zeta potentials of PANi(ES), TiO_2 and the PANi(ES^+)/TiO_2(O^-) composite in different pH and their pH of zero-point charge; TGA of PANi(ES), TiO_2 and the PANi(ES)/TiO_2(O^-) composite before (c) and after (d) adsorption of Pb^{2+}, Zn^{2+} and Cu^{2+}; (e) XRD spectra of PANi(ES), TiO_2 and the PANi(ES^+)/TiO_2(O^-) composite; (f) N_2 adsorption and desorption isotherms of PANi(ES), TiO_2 and the PANi(ES^+)/TiO_2(O^-) composite; SEM (g) and TEM (h) image; TEM-EDS mapping image(i).

Table 1
Assignments of the FT-IR absorptions for PANi, TiO_2 and the PANi/TiO_2 composite before and after adsorption with Pb^{2+}, Zn^{2+} and Cu^{2+}.

Wavenumber (cm^{-1})											Assignments [12]
Before adsorption			After adsorption								
PANi	TiO_2	PANi/TiO_2	PANi/TiO_2 Pb^{2+}	PANi/TiO_2 Zn^{2+}	PANi/TiO_2 Cu^{2+}	TiO_2 Pb^{2+}	TiO_2 Zn^{2+}	TiO_2 Cu^{2+}	PANi Pb^{2+}	PANi Zn^{2+}	PANi Cu^{2+}	
–	3419	3728	3728	3728	3728	3519	3547	3436	–	–		NH_2 stretching vibration
3226	–	3222	3223	3225	3218	–	–	–	3225	3228	3228	H-bonded NH str.
2981	–	3047	3045	3048	3047	–	–	–	2980	2981	2980	Sum frequency or impurity
–	1629	–	–	–	–	1621	1619	1625	–	–	–	-OH in-plane bending vibration
1565	–	1581	1579	1581	1576	–	–	–	1562	1563	1563	N=Q=N
1482	–	1498	1498	1498	1498	–	–	–	1484	1476	1486	NH-B-NH
1384	–	1380	1380	1380	1380	1380,1375	1380,1375	1380	1384	1384	1384	C-N str. In QBQ or NO_3^-
–	–	1353	1353	1353	1351	–	–	–	–	–	–	C-H aromatic bending vibration
1295		1301	1301	1301	1301	–	–	–	1295	1295	1295	C-N str. In QBQ, QBB, BBQ
1240	–	1247	1247	1247	1247	–	–	–	1240	1240	1240	C_β-H in-plane bending vibration
–	–	1170	1170	1170	1170	–	–	–	–	–	–	A model of N=Q=N
1131	–	1143	1146	1146	1145	–	–	–	1123	1123	1123	A model of $Q=N^+H$-B or B-NH-B
*	–	1040, 960, 822, 797, 690, 560				–	–	–	1060, 960, 830, 740, 690, 530*			C-H bending of benzene ring
–	–	–	–	–	834	–	–	834				Cu^{2+} [2]
–	–	–	–	828	–	–	828	–				Zn^{2+} [31]
–	–	–	720	–	–	720	–	–				Pb^{2+} [9]
–	400-700	400-700	400-700	400-700	400-700	400-700	400-700	400-700	–	–		O–Ti–O [27]

follows:

$$Q_e = \frac{(C_0 - C_e)V}{m} \quad (1)$$

$$\text{Recycle efficiency} = \frac{Q_{e,n}}{Q_{e,0}} \times 100\,\% \quad (2)$$

where Q_e ($mg{\cdot}g^{-1}$) represents the equilibrium adsorption capacity; C_0 and C_e ($mg{\cdot}L^{-1}$) represents the initial and equilibrium concentrations of heavy metal ions, respectively; V (L) represents the volume of the solution; m (g) represents the weight of adsorbent; $Q_{e,n}$ represents the adsorption capacity at n^{th} cycle; $Q_{e,0}$ represents the adsorption capacity at the start of the experiment.

3. Results and discussion

3.1. Characterization

Fig. 1(a) illustrates the FT-IR spectra of the PANi/TiO_2 composite together with that of PANi and TiO_2, and the assignments of the characteristic absorption peaks are displayed in Table 1. The spectrum of the PANi/TiO_2 composite contains the characteristic peaks of both PANi and TiO_2, showing the successful combination of PANi and TiO_2 in the PANi/TiO_2 composite. The strong peaks at 3419 and 1629 cm^{-1}, which are assigned to hydroxyl in the spectrum of TiO_2, suggests that TiO_2 is mainly synthesized as TiO_2(OH) [27]. It is also clear in the spectra of both PANi and the PANi/TiO_2 composite that the synthesized PANi is in the emeraldine state (ES), with nearly similar intensity for the 1580 cm^{-1} and 1498 cm^{-1} peak, associated to the quinoid ring and benzenoid ring, respectively [12]. The broadening peak at around 1140 cm^{-1}, which resulted from some degree of electron delocalization, further implies PANi is in the emeraldine salt (ES) state [12]. Literature reviews show that numerous attempts have been made to modify substrates with PANi [28–30]. Among them, the surface functionalization can be achieved by surface graft copolymerization with groups such as acrylic acid [29]. The interfacial charge transfer interactions between an acrylic acid functionalized substrate and PANi can be then obtained through doping. Herein, identified peak shifts are observed at 3419 and 1629 cm^{-1}, which are assigned to OH^-, and 1565 and 1482 cm^{-1}, which are ascribed to doping sites of ES, giving further evidence that $TiO_2(O^-)$ is acting as a dopant for PANi in the same manner as NO_3^- [12]. PANi should act as a p-type polymer when doped and donates its electron cloud density to $TiO_2(O^-)$, making $TiO_2(O^-)$ into an n-type dopant in the PANi/TiO_2 composite. This charge transfer (CT) interaction would result in the electron cloud density change around aniline ring and TiO_2 as well as the peak shift of the aniline ring and hydroxyl in their FT-IR spectra.

In order to further verify the doping nature of $TiO_2(O^-)$ on $PANi^+$, PANi/TiO_2 was synthesized using a Buchwald-Hartwig reaction. This experiment further supports the suggestion that $TiO_2(O^-)$ behaves as a dopant because the reaction was conducted in an alkaline NaOtBu solution, and no additional dopant ions were introduced. After the composite was dried, a light green solid was obtained. The solid was collected and investigated using solid UV–vis NIR spectrometry and FT-IR, shown in Fig. ***S1***. The PANi was confirmed to be in the ES state because in addition to the peaks with similar intensity at 1580 cm^{-1} and 1498 cm^{-1} in FT-IR, a broad conductive peak at around 700 nm and a peak at 1123 cm^{-1} were observed respectively in the solid Uv-*vis* NIR and FT-IR spectra, readily confirming that $TiO_2(O^-)$ is a dopant of PANi. However, these peaks could not be observed in the spectra of PANi without TiO_2. In addition, the color of the PANi prepared without TiO_2 changed from yellow brown to blue after it was exposed to air, suggesting an undoped state of the PANi. The CT interaction between PANi and TiO_2 proposed herein (Scheme 1) would explain the mechanism of the synergistic adsorption between PANi and TiO_2 for the selective adsorption of heavy metals discussed in the later section.

The p-type doping was also confirmed by zeta potential investigations shown in Fig. 1(b). The pH of zero-point charge (pH_{pzpc}) for the composite is given as 8.25, which is slightly lower than that of PANi (8.41), implying that the PANi in the composite remains in the ES state when the pH is lower than 8.25. However, the degree of doping, which can be reflected by the zeta potential, gradually decreased with the increase in pH, showing the metastable state of the ES in aqueous solution. In addition to the dedoping of ES in aqueous solution, the ES was also affected by the hydrolysis caused by H_2O and dissolved oxygen, and would decompose gradually to form more the benzoquinone

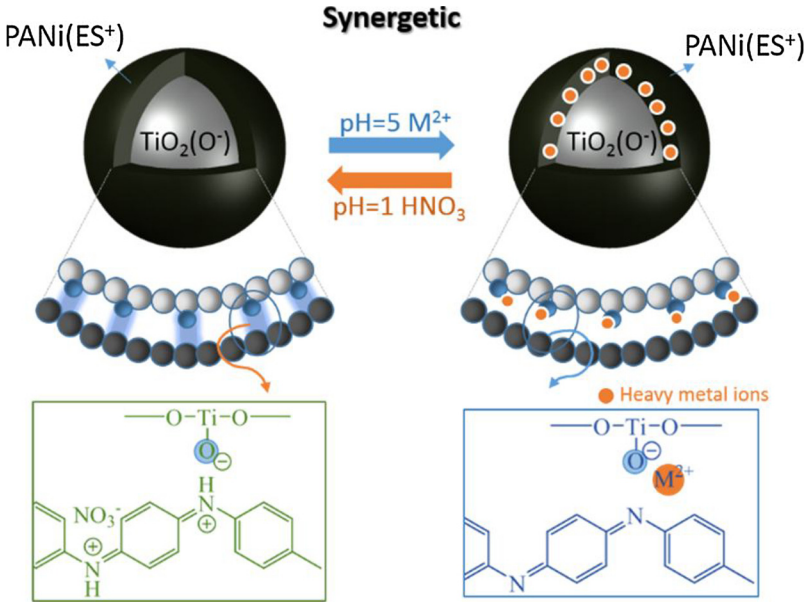

Scheme 1. The synergistic adsorption between ES and TiO_2 in the PANi(ES^+)/TiO_2(O^-) composite for the selective adsorption for heavy metal ions.

groups, thus reducing the degree of oxidation in ES [32]. The dedoping process discussed herein (Scheme 1) would also be the basis for the mechanism of the synergistic adsorption between PANi and TiO_2 in the selective adsorption of heavy metals discussed in the later section.

The comparison of thermal decomposition for the PANi(ES^+)/TiO_2(O^-) composite before and after PANi modification and heavy metal adsorption are depicted in Figs. 1(c) and (d). The textural properties of PANi, TiO_2 and the PANi/TiO_2 composite before and after adsorption are also listed in Table 2. Before the PANi modification, TiO_2 clearly shows two major weight-loss transitions at around 100 °C and 400 °C, which can be ascribed to the loss of adsorbed water and hydroxyls [33]. Meanwhile, we can ascribe a three-stage process to the thermal degradation of PANi(ES^+) and the PANi(ES^+)/TiO_2(O^-) sample according to previous research [10,11]. The first weight loss from room temperature to 100 °C is assigned to the loss of physically and chemically adsorbed water, and the second weight loss interval between 100 °C and 450 °C is ascribed to the loss of the doping ions including the hydroxyls on TiO_2(O^-) and NO_3^- in the doping chain. The final weight loss above 450 °C is ascribed to the further thermal decomposition of PANi [12,13]. F. A. Rafiqi et al. [34] indicated in their investigation of the thermal stability of PANi that the decomposition and the glass transition temperature (T_g) can be considerably enhanced by the strong electrostatic interactions between the ions and the PANi chains. It can be noted that the second weight loss interval for the ions dedoping from the ES extends from 350 °C to 450 °C after ionic doping with TiO_2(O^-), suggesting the CT interaction between TiO_2(O^-) and PANi [34]. It is therefore reasonable to ascribe the second interval to the loss of dopant ions, and the thermo-stability reduces as the loss of dopants. To verify the property that dedoping of dopant from ES may occur in aqueous solution of pH = 5, the TGA investigation on the composite after treatment of pH = 5 water or after adsorption of Pb^{2+}, Zn^{2+} and Cu^{2+} were conducted. It is encouraging to observe that the weight of the composite reduces after adsorption of Pb^{2+}, Zn^{2+} and Cu^{2+}, and the thermal stabilities of the polymer are greatly reduced (decomposing temperature lowers from 421 °C to around 180 °C). Furthermore, from the TGA curve of the composite after being immersed in a pH = 5 water solution, loss of the dopant is observed when compared to the weight loss of the composite before dipping at the second interval. The decomposition temperature also reduces from 421 to 385 °C due to the loss of stabilization from the dopant. These studies further support the conclusion suggested in the zeta potential study that the dedoping process of ES must occur in the heavy metal solution with pH = 5.

Table 2
The proportion of each component in PANi, TiO_2 and the PANi/TiO_2 composite before and after water or heavy metal solution treatment.

	Temperature		
	< 100 °C (Water/ Hydroxyl)	100–450 °C (Hydroxyl/Doping ions)	> 450 °C (PANi)
PANi	7.06 w·w^{-1}% (Water)	19.10 w·w^{-1}% (Doping ions)	28.85 w·w^{-1}% (PANi)
TiO_2	14.57 w·w^{-1}% (Water/Hydroxyl)		–
PANi/TiO_2	5.04 w·w^{-1}% (Water/ Hydroxyl)	15.80 w·w^{-1}% (Hydroxyl/Doping ions)	24.59 w·w^{-1}% (PANi)
PANi/TiO_2 Pb^{2+}	6.62 w·w^{-1}% (Water/ Hydroxyl)	8.94 w·w^{-1}% (Hydroxyl/Doping ions)	16.03 w·w^{-1}% (PANi)
PANi/TiO_2 Zn^{2+}	3.27 w·w^{-1}% (Water/ Hydroxyl)	11.61 w·w^{-1}% (Hydroxyl/Doping ions)	17.65 w·w^{-1}% (PANi)
PANi/TiO_2 Cu^{2+}	3.26 w·w^{-1}% (Water/ Hydroxyl)	9.06 w·w^{-1}% (Hydroxyl/Doping ions)	18.57 w·w^{-1}% (PANi)
PANi/TiO_2 pH = 5 water solution	5.04 w·w^{-1}% (Water/ Hydroxyl)	11.26 w·w^{-1}% (Hydroxyl/Doping ions)	25.20 w·w^{-1}% (PANi)

Fig. 1(e) displays the XRD pattern of TiO_2 and the PANi(ES^+)/TiO_2(O^-) composite. For TiO_2, typical crystalline peaks at 2-theta of 25.3°, 37.8° and 48.1° ascribed to the anatase TiO_2 are shown in the pattern [35]. However, the intensity of these peaks decreases considerably after combination with amorphous PANi, suggesting that the TiO_2 is coated with PANi [36]. This theory is also evidenced by the N_2 adsorption desorption isotherm study shown in Fig. 1(f) and Table 3. The surface area and pore volume of the TiO_2 decrease after coating with PANi, which results from the covering and blocking by PANi, confirming the core-shell structure of the PANi(ES^+)/TiO_2(O^-) composite [37]. It is also interesting to note that the shape of the isotherm of TiO_2 is changed from Type II to Type I after modification, suggesting the reshaping of the pore structure of TiO_2 by PANi.

SEM, SEM-EDS mapping, TEM and TEM-EDS mapping investigation were also conducted to further verify the structure. From the SEM

Table 3
The textural properties of PANi, TiO_2 and the PANi/TiO_2 composite before and after adsorption.

Composites	S_{BET} ($m^2 \cdot g^{-1}$)	V ($cm^3 \cdot g^{-1}$)	R(Å)
PANi	38.44	0.302	112.7
TiO_2	163.36	0.37	39.5
PANi /TiO_2	9.85	0.134	104.1
PANi /TiO_2 Pb^{2+}	7.67	0.0815	59.7
PANi /TiO_2 Zn^{2+}	10.76	0.105	102.1
PANi /TiO_2 Cu^{2+}	8.94	0.105	66.5

results shown in Fig. 1(g), a typical mushroom shape was observed. A certain degree of aggregation was also confirmed from the image. SEM-EDS mapping images shown in Fig. ***S***3 show good overlapping of N and Ti, indicating that there is not isolated TiO_2 or PANi acquired during the synthesis. This good combination of PANi and TiO_2 may result from the strong doping and interaction between PANi and TiO_2. To further confirm the core-shell structure of PANi/TiO_2, TEM and TEM-EDS mapping were carried out. The thickness of PANI shell was estimated to be 5 nm in the chosen particle from the TEM image in Fig. 1(h). However, it should be noted that the thickness could not be uniform because the thickness was very hard to be controlled during the synthesis. It can be clear detected that the element Ti was completely covered by N and C in the EDS mapping images in Fig. 1(i), and, furthermore, core TiO_2 with lattice fringes could be seen to be wrapped by shell PANi which is amorphous in the TEM image in Fig. 1(h), further suggesting the core-shell structure of the PANi/TiO_2 composite. However, an aggregation of TiO_2 with a size of 100 nm was observed in the TEM image shown in Fig. ***S4***, indicating that the structure is not a perfect core-shell structure. Nevertheless, the TiO_2 is still well wrapped by PANi, providing a good condition for the synergetic effect between PANi and TiO_2 for the selective adsorption.

3.2. Adsorption experiments

The adsorption kinetic study was carried out and is shown in the ***Supplementary Material***. The kinetic study, which can be well predicted by a pseudo-second-order model and a multi-linear Weber-Morris model, exhibits a rapid adsorption of the Pb^{2+}, Zn^{2+} and Cu^{2+} within 40 min, 5 min and 5 min, respectively. The recyclable adsorption capacity can be also applied in the field investigation, showing a promising future if applied in adsorption applications.

The isotherm, which describes the relationship between the initial metal ion concentration and the adsorption capacity of adsorbents, was applied to illuminate the selective adsorption properties of the composite. It can also be applied to describe the adsorption capacity, selectivity and affinity of the adsorbent towards certain heavy metal ions in a multiple metal ion system, which is important but rarely conducted. In the present study, the isotherm data were fitted and described using typical Langmuir [38] and Freundlich models [39] to demonstrate the adsorption affinity and capacity, while using Dubinin-Radushkevich [40] and Temkin models [41] to estimate the adsorption free energy and heat [42,43]. Relevant fitting parameters and details about the models are given in Tables 4 and ***S1***, while their graphical representation is plotted in Figs. 2 and ***S5-6***. As can be seen in the table, the adsorption isotherms for Pb^{2+}, Zn^{2+} and Cu^{2+} can be well described by the Langmuir model, followed by the Freundlich and Temkin models in all cases, while the Dubinin-Radushkevich model has the lowest applicability when predicting these adsorptions either in the single or multiple metal ion system. This indicates that the single and competitive adsorption of heavy metal ions onto the composite is generally monolayer, and adsorption sites on the surface of the PANi (ES^+)/TiO_2(O^-) composite are homogenously distributed [7,9,37,38].

From the Langmuir result, the adsorption capacities of PANi towards heavy metals, unexpectedly, reduced after combination of TiO_2. In addition, the adsorption capacities of PANi towards Zn^{2+} and Cu^{2+}, interestingly, increased almost two times in the competition system. The reduce of adsorption capacities can be ascribed to the addition of TiO_2, which have lower adsorption capacities. However, the increase of adsorption capacities in the competition system may result from the synergistic action between heavy metals. High ionic concentration may increase the pore size of PANi, resulting in better availability of the adsorption sites than in single ion solution [19].

The monolayer adsorption capacity of the composite towards Pb^{2+}, Zn^{2+} and Cu^{2+} obtained from the Langmuir model are calculated to be 0.460 $mmol \cdot g^{-1}$ (95.40 $mg \cdot g^{-1}$) for Pb^{2+}, 0.594 $mmol \cdot g^{-1}$ (38.62 $mg\,g^{-1}$) for Zn^{2+} and 0.140 $mmol \cdot g^{-1}$ (9.00 $mg\,g^{-1}$) for Cu^{2+}, respectively at 25 °C in the single metal ion system, which exhibits competitive adsorption capacities for Pb^{2+} and Zn^{2+} compared to other adsorbents shown in Table ***S2***. The adsorption capacities for Pb^{2+} and Zn^{2+} also show a positive correlation with temperature, which is often observed in some ionic exchange adsorption [44]. Interestingly, the adsorption capacity of Cu^{2+} displays a slight decrease with the temperature, indicating a different adsorption mechanism than that of Pb^{2+} and Zn^{2+}.

The selectivity and affinity of the PANi(ES^+)/TiO_2(O^-) composite towards certain heavy metal ions was further investigated in multiple metal ion systems. To illustrate the adsorption selectivity, the ***P*** factor, which is a dimensionless parameter shown in Eq. (3), is introduced.

$$\boldsymbol{P} = \frac{Q_{max,single}}{Q_{max,multiple}} \tag{3}$$

Where, $Q_{max,single}$ and $Q_{max,multiple}$ are the maximum adsorption capacities for heavy metals acquired by Langmuir model in the single and multiple metal ion systems. Specifically, the higher the affinity towards one metal the composite has, the closer the value of ***P*** to 1 will be; The higher selectivity the composite has, the bigger the difference in the ***P*** values for different metal ions will be. The ***P*** values of the composite to three heavy metals are recorded in Table 4. It is interesting that the ***P*** values show a descending trend of $Zn^{2+} > Pb^{2+} > > Cu^{2+}$, where the adsorption of Cu^{2+} is almost suppressed in the competition adsorption, suggesting that the PANi(ES^+)/TiO_2(O^-) composite has impressive selectivity. Therefore, even though the adsorption capacities of PANi reduced after being composited with TiO_2, the impressive selectivity was tuned and achieved. The trade-off was believed to be meaningful because the composite with high selectivity can be applied in the heavy metal ion separation, achieving the recycling of the heavy metal ions. In addition, this result challenges the conclusions of the majority of publications that the main mechanism of the selective adsorption is mainly related to the properties of the heavy metals such as ionic radii, Pauling electronegativity and standard reduction potential [11,45]. The publications contradict each other and cannot explain all the experimental phenomena satisfactorily (***i.e.*** Herein, Zn^{2+} has smaller ionic radii and Pauling electronegativity (0.74 nm and 1.65, respectively) than Pb^{2+} (0.97 nm and 2.33, respectively) and Cu^{2+} (0.7 nm and 1.9, respectively), but it has larger affinity.). The detailed synergistic adsorption mechanism will be discussed in the later section.

The results of the Dubinin-Radushkevich and Temkin models listed in Table ***S1***, poorly fit to the data, therefore the value of the adsorption free energy (***E***) and heat (***B***) are not suitable to determine the adsorption mechanism.

3.3. Mechanism

In the previous characterization, it was found that the metal oxide with hydroxyl on the surface would act as a dopant for the polymer in a polymer/metal oxide composite. However, the doped state of polymers including polypyrrole, polyaniline and polythiophene could be unstable and very easy to dedope once in aqueous solutions with high pH (> 3) [12,13,32]. Y. Li [13] pointed out that among these polymers,

Table 4
Single and multi-component adsorption isotherms parameters describing the adsorption of heavy metals (Pb^{2+}, Zn^{2+}, Cu^{2+}) onto the PANi/TiO_2 composite, on the basis of Langmuir and Freundlich models.

			PANi /TiO_2									PANi			TiO_2		
			Pb^{2+}			Zn^{2+}			Cu^{2+}			Pb^{2+}	Zn^{2+}	Cu^{2+}	Pb^{2+}	Zn^{2+}	Cu^{2+}
			15 °C	25 °C	45 °C	15 °C	25 °C	45 °C	15 °C	25 °C	45 °C	25 °C	25 °C	25 °C	25 °C	25 °C	25 °C
Langmuir	**Single-component**	$Q_{m,mass}$	94.80	95.24	96.15	34.48	38.62	51.55	18.20	9.00	6.75	270.27	77.95	37.62	68.13	46.83	15.63
		$Q_{m,mol}$	0.459	0.460	0.464	0.530	0.594	0.793	0.284	0.140	0.105	1.305652	1.199231	0.587813	0.329	0.720	0.244
		K_L	0.00617	0.00726	0.00985	0.0692	0.0701	0.477	0.00998	0.0101	0.0178	0.0035	0.0045	0.00254	0.020	0.0029	0.0010
		R^2	0.980	0.985	0.985	0.983	0.980	0.997	0.992	0.994	0.982	0.999	0.999	0.999	0.980	0.994	0.997
	Multi-component	$Q_{m,mass}$	–	67.04	–	–	35.59	–	–	0	–	232.56	232.56	160.33	45.38	45.12	0
		$Q_{m,mol}$	–	0.324	–	–	0.547	–	–	0	–	1.123	3.578	2.504	0.219	0.694	0
		K_L	–	0.030	–	–	0.00673	–	–	–	–	0.00952	0.00474	0.00635	0.0039	0.0022	–
		R^2	–	0.979	–	–	0.963	–	–	–	–	0.974	0.984	0.993	0.998	0.999	–
		P	–	**0.707**	–	–	**0.922**	–	–	**0**	–	**0.860**	**2.98**	**4.26**	**0.666**	**0.963**	**0**
Freundlich	**Single-component**	K_F	5.774	7.428	9.608	9.972	11.280	11.167	1.312	0.588	1.181	4.749	1.725	0.393	16.66	0.58	0.10
		$1/n$	0.405	0.374	0.338	0.208	0.207	0.235	0.398	0.430	0.268	0.586	0.562	0.642	0.21	0.62	0.80
		R^2	0.968	0.874	0.981	0.875	0.884	0.898	0.913	0.956	0.953	0.984	0.976	0.985	0.744	0.971	0.790
	Multi-component	K_F	–	9.789	–	–	2.049	–	–	–	–	6.493	5.156	6.193	1.15	0.30	–
		$1/n$	–	0.334	–	–	0.429	–	–	–	–	0.616	0.577	0.495	0.64	0.72	–
		R^2	–	0.981	–	–	0.829	–	–	–	–	0.960	0.971	0.9321	0.995	0.997	–

Langmuir model: $Q_e = \frac{Q_m K_L C_e}{1 + K_L C_e}$, $P = \frac{Q_{max,single}}{Q_{max,multiple}}$.

Q_e (mg·g^{-1}) is the adsorption capacity; $Q_{m,mass}$ (mg·g^{-1})/$Q_{m,mol}$ (mmol·g^{-1}) represents the maximum adsorption capacity in mass and mole unit; K_L (L·mg^{-1}) is an Langmuir constant relate to the affinity between adsorbents and adsorbate; ***P*** factor is a dimensionless parameter to estimate the selectivity for heavy metals.

Freundlich model: $Q_e = K_F C_e^{1/n}$.

K_F (mg^{1-n}·L^n·g^{-1}) is a constant related to the adsorption capacity of adsorbent when the equilibrium metal ions concentration equals to 1; n states the degree of dependence of the adsorption on the equilibrium concentration.

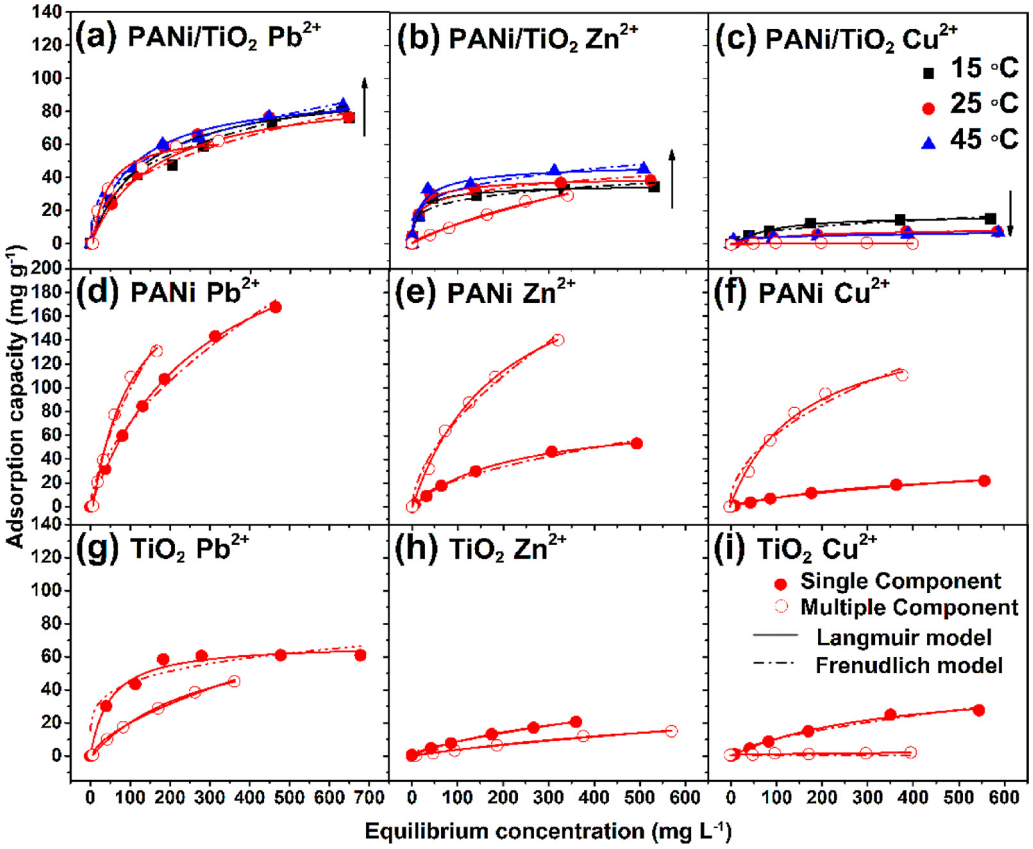

Fig. 2. Single and multi-component adsorption isotherms for the adsorption of Pb^{2+}, Zn^{2+} and Cu^{2+} onto the PANi(ES^+)/TiO_2(O^-) composite (a–c), PANi(ES) (d–f) and TiO_2 (g–i), fitting with Langmuir and Freundlich model.

polythiophene has the lowest doping stability in aqueous solutions, and undergoes total dedoping even at neutral pH, followed by polyaniline and polypyrrole. Several investigations conducted by E.T Tang et al. [12] also demonstrated that polyaniline (ES) could not retain in the doped state in aqueous solution with pH > 4. Therefore, for the PANi (ES^+) composite doped with TiO_2(O^-), the hydroxyls on the TiO_2, which has smaller radius than NO_3^-, can be dedoped in advance when the composites are dosed into the solution (pH = 5). In the meantime, the cationic heavy metal ions would dope the TiO_2(O^-) to keep it electrically neutral. Thus, the adsorption affinity and selectivity towards heavy metal ions will be determined by TiO_2(O^-). This hypothesis is strongly supported by the results obtained in the heavy metal ion adsorption study of the PANi(ES^+)/TiO_2(O^-) composite, in which the dedoping process is observed and the selective order for the heavy metal ion adsorption of the composite has the same pattern of Zn^{2+} > Pb^{2+} > > Cu^{2+} as TiO_2.

To further confirm this hypothesis for the selective adsorption of the PANi(ES^+)/TiO_2(O^-) composite, we conducted FT-IR spectra investigations after adsorption. The results are depicted in Fig. S2 and Table 1. For TiO_2, the peaks assigned to the hydroxyls at 3419 cm^{-1} and 1629 cm^{-1} show an obvious red shift to higher wavenumbers after adsorbing Pb^{2+}, Zn^{2+} and Cu^{2+}, suggesting the hydroxyls on the surface of TiO_2 could interact with heavy metals after dedoping [46]. However, it can be clearly seen that the peak shift for Cu^{2+} is relatively smaller than the other two ions. In addition, there is a peak situated at 1375 cm^{-1} that is absent in the spectrum of Cu^{2+} adsorbed TiO_2, and is prominent in the spectra of Pb^{2+} and Zn^{2+} adsorbed TiO_2. This suggests there is a favorable adsorption mechanism occurring in the Pb^{2+} and Zn^{2+} adsorption, resulting in the generation of the peak at 1375 cm^{-1}, which is unfavorable for Cu^{2+} adsorption. In the PANi(ES) spectra and the PANi(ES^+)/TiO_2(O^-) composite spectra, it can be noted that the peaks assigned to the quinoid ring shift after adsorption, indicating the dedoping or the interaction between metal ions and the quinoid ring [12,47]. However, after Cu^{2+} adsorption, a notable decrease in the intensity of the peak at 1565 cm^{-1} (assigned to the quinoid ring) can be clearly detected in the spectrum of PANi(ES) but cannot be detected in the spectrum of the PANi(ES^+)/TiO_2(O^-) composite. The number of quinoid rings and benzenoid rings can be quantitatively determined by the intensity of peak situated at 1580 cm^{-1} and 1498 cm^{-1} [47]. The spectrum of pristine LM powder exhibits a very low intensity ratio of the 1580 cm^{-1} to 1498 cm^{-1} peaks, while that of NA shows an high intensity ratio of the 1580 cm^{-1} to 1498 cm^{-1} peaks which is larger than 1 [12]. Hydrolysis can reduce this ratio by decomposing the PANi into benzoquinone. Additionally, some reductants can also reduce the degree of oxidation in PANi [48]. Herein, there must be an unknown mechanism of interaction between PANi and Cu^{2+}, which would reduce the number of the quinoid rings as well as the degree of oxidation in PANi. However, this interaction is forbidden after $PANi^+$ is doped with TiO_2(O^-), which supports the conclusion that Cu^{2+} may be unfavorable for TiO_2 to some extent.

To summarize, we propose a synergistic adsorption mechanism for polymer/metal oxide composite on the selective adsorption herein. In the PANi(ES^+)/TiO_2(O^-) composite, TiO_2(O^-) acts as a dopant that dopes the polymer chain through hydroxyls during synthesis. Dedoping will occur due to the metastability of the doped state of the composite in a non-acid solution (pH = 5), resulting the hydroxyls on the TiO_2 to dedope in advance. Meanwhile, the cationic heavy metal ions would then dope the TiO_2(O^-) to keep it electrically neutral. Thus, the adsorption affinity and selectivity towards heavy metal ions will be determined by TiO_2.

This synergistic mechanism can be also verified by studying the effect of the solution pH on the adsorption (depicted in Fig. 3). The results show that the adsorption capacities for Pb^{2+}, Zn^{2+} and Cu^{2+} increase with the increased pH, which also supports the synergistic

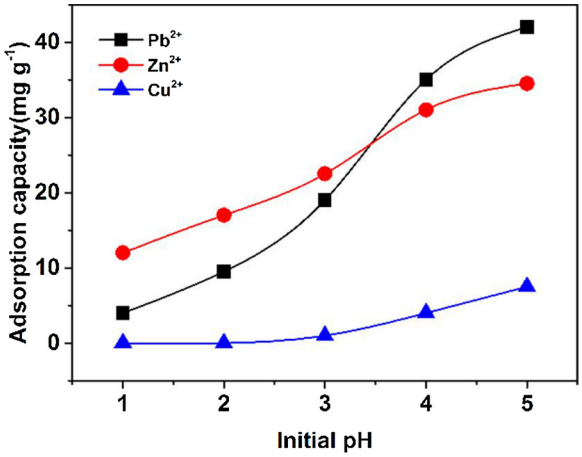

Fig. 3. The adsorption capacities of the PANi(ES^+)/TiO_2(O^-) composite for Pb^{2+}, Zn^{2+} and Cu^{2+} in different initial solution pH.

mechanism we proposed well. Specifically, the dedoping process would be greatly suppressed by the high concentration of H^+, resulting in the unavailability of adsorption sites on TiO_2 [12]. Moreover, limited imine sites could be produced by low pH, which may also reduce the adsorption capacity.

4. Conclusions

The emeraldine salt doped with $TiO_2(O^-)$ and NO_3^- was synthesized to provide new experimental evidence to support the hypothesis proposed for the synergistic mechanism between a polymer and metal oxide and the selective adsorption for heavy metal ions (Pb^{2+}, Zn^{2+}, Cu^{2+}). Characterizations including FT-IR, zeta potential analysis, TGA, XRD, N_2 adsorption desorption isotherm, SEM-EDS and TEM-EDS confirm that the emeraldine salt, in its oxidized p-type doping state, is coated on the surface of the TiO_2(OH), which is in the n-type state, forming a charge-transfer heterojunction structure. This composite was further studied by single metal and multiple metal adsorption experiment to get insight into the selective adsorption mechanism. The adsorption capacities reach 0.594 mmol·g^{-1}, 0.460 mmol·g^{-1} and 0.140 mmol·g^{-1}, respectively in single metal system and reach 0.547 mmol·g^{-1}, 0.324 mmol·g^{-1} and 0 mmol·g^{-1}, respectively in multi metal system with ***P*** values reach 0.922, 0.707 and 0, respectively for Zn^{2+}, Pb^{2+} and Cu^{2+}, exhibiting a special affinity order of $Zn^{2+} > Pb^{2+} > > Cu^{2+}$, and the adsorption for Cu^{2+} is completely suppressed in the multiple metal system. The ***P*** values of TiO_2, which are 0.963, 0.666 and 0 for Zn^{2+}, Pb^{2+} and Cu^{2+}, respectively, follow the same trend with PANi/TiO_2 composite. These experimental results together with characterization results obtained from FT-IR and TGA provide reliable evidence for the synergistic mechanism we proposed. $TiO_2(O^-)$ will behave as dopant doping the PANi(ES^+) through hydroxyls. The metastability of the doping state of PANi in a non-acid solution (pH = 5) results in the selective adsorption of metal ions on $TiO_2(O^-)$. The adsorption affinity and selectivity towards heavy metal ions is determined by TiO_2. This mechanism we proposed herein explains the selective properties of the polymer/TiO_2 composite system, and it would also explain the contradictions that were noted in other investigations of the selectivity. It can also guide the design of an adsorbent with expected selective properties for the adsorption engineering. However, the reason why TiO_2 has special adsorption affinity to Zn^{2+} and poor affinity to Cu^{2+} remains unknown. More experimental evidence for this mechanism using other polymer/metal oxide composites needs to be obtained. The relevant investigations will be designed and conducted in our further work.

Acknowledgements

The authors gratefully acknowledge Dr. Jean-Charles Eloi from Chemical Imaging Facility in University of Bristol for the SEM and TEM investigation and analysis, and Esther Townsend for her kind help with the language and her helpful suggestions to improve the quality of our paper. The authors gratefully acknowledge the Shaanxi Key research and development projects, China (Grant No. 2017SF-386), the Fundamental Research Funds for the Central Universities of China and the financial supports from the National Natural Science Foundation of China (Grant No. 21307098).

Appendix A. Supplementary data

Supplementary material related to this article can be found, in the online version, at doi: https://doi.org/10.1016/j.synthmet.2018.08.006.

References

[1] T. Trakulsujaritchok, N. Noiphom, N. Tangtreamjitmun, R. Saeeng, Adsorptive features of poly(glycidyl methacrylate-co-hydroxyethyl methacrylate): effect of porogen formulation on heavy metal ion adsorption, J. Mater. Sci. 46 (2011) 5350–5362.
[2] J. Li, J. Tong, X. Li, Z. Yang, Y. Zhang, G. Diao, Facile microfluidic synthesis of copolymer hydrogel beads for the removal of heavy metal ions, J. Mater. Sci. 51 (2016) 10375–10385.
[3] G. Macchi, D. Marani, M. Pagano, G. Bagnuolo, A bench study on lead removal from battery manufacturing wastewater by carbonate precipitation, Water Res. 30 (1996) 3032–3036.
[4] A. Dąbrowski, Z. Hubicki, P. Podkościelny, E. Robens, Selective removal of the heavy metal ions from waters and industrial wastewaters by ion-exchange method, Chemosphere 56 (2004) 91–106.
[5] F. Fu, Q. Wang, Removal of heavy metal ions from wastewaters: a review, J. Environ. Manage. 92 (2011) 407–418.
[6] H.R. Mortaheb, A. Zolfaghari, B. Mokhtarani, M.H. Amini, V. Mandanipour, Study on removal of cadmium by hybrid liquid membrane process, J. Hazard. Mater. 177 (2010) 660–667.
[7] J. Chen, N. Wang, H. Ma, J. Zhu, J. Feng, W. Yan, Facile modification of a polythiophene/TiO_2 composite using surfactants in an aqueous medium for an enhanced Pb(II) adsorption and mechanism investigation, J. Chem. Eng. Data 62 (2017) 2208–2221.
[8] R. Karthik, S. Meenakshi, Removal of Pb(II) and Cd(II) ions from aqueous solution using polyaniline grafted chitosan, Chem. Eng. J. 263 (2015) 168–177.
[9] J. Chen, J. Feng, W. Yan, Facile synthesis of a polythiophene/TiO_2 particle composite in aqueous medium and its adsorption performance for Pb(II), RSC Adv. 5 (2015) 86945–86953.
[10] J. Gao, S.P. Sun, W.P. Zhu, T.S. Chung, Chelating polymer modified P84 nanofiltration (NF) hollow fiber membranes for high efficient heavy metal removal, Water Res. 63 (2014) 252–261.
[11] R. Karthik, S. Meenakshi, Chemical modification of chitin with polypyrrole for the uptake of Pb(II) and Cd(II) ions, Int. J. Biol. Macromol. 78 (2015) 157–164.
[12] E.T. Kang, K.G. Neoh, K.L. Tan, Polyaniline: a polymer with many interesting intrinsic redox states, Prog. Polym. Sci. 23 (1998) 277–324.
[13] Y. Li, Conducting Polymers, Springer International Publishing, 2015.
[14] M.H. Qomi, H. Eisazadeh, M. Hosseini, H.A. Namaghi, Manganese removal from aqueous media using polyaniline nanocomposite coated on wood sawdust, Synthetic Met. 194 (2014) 153–159.
[15] H.B. Bradl, Adsorption of heavy metal ions on soils and soils constituents, J. Colloid. Interf. Sci. 277 (2004) 1–18.
[16] J. Wu, D.A. Laird, M.L. Thompson, Sorption and desorption of copper on soil clay components, J. Environ. Qual. 28 (1999) 334–338.
[17] R.M. McKenzie, The adsorption of lead and other heavy metals on oxides of manganese and iron, Aust. J. Soil Res. 18 (1980) 61–73.
[18] D.C. Adriano, Trace elements in terrestrial environments, Q. Rev. Biol. 32 (1986) 374.
[19] V. Gilja, K. Novaković, J. Travas-Sejdic, Z. Hrnjak-Murgić, M. Kraljić Roković, M. Žic, Stability and synergistic effect of polyaniline/TiO_2 photocatalysts in degradation of azo dye in wastewater, Nanomaterials 7 (2017) 412.
[20] X. Li, C. Shi, J. Wang, J. Wang, M. Li, H. Qiu, H. Sun, K. Ogino, Polyaniline-doped TiO_2/PLLA fibers with enhanced visible-light photocatalytic degradation performance, Fiber. Polym. 18 (2017) 50–56.
[21] V. Mohammad, A. Somayeh, O. Mohammadreza, Z.M. Abdolsamad, Synthesis, characterization and optimization of N-TiO_2/PANI nanocomposite for photodegradation of acid dye under visible light, Polym. Composite (2017), https://doi.org/10.1002/pc.24574 in press.
[22] S.A. Nabi, M. Shahadat, R. Bushra, A.H. Shalla, Heavy-metals separation from industrial effluent, natural water as well as from synthetic mixture using synthesized novel composite adsorbent, Chem. Eng. J. 175 (2011) 8–16.
[23] S. Piri, F. Piri, B. Rajabi, S. Ebrahimi, A. Zamani, M.R. Yaftian, In situ one-pot

electrochemical synthesis of aluminum oxide/polyaniline nanocomposite; characterization and its adsorption properties towards some heavy metal ions, J. Chin. Chem. Soc. Taip. 62 (2015) 1045–1052.
[24] Q. Zhang, X. Du, X. Ma, X. Hao, G. Guan, Z. Wang, C. Xue, Z. Zhang, Z. Zuo, Facile preparation of electroactive amorphous α-ZrP/PANI hybrid film for potential-triggered adsorption of Pb^{2+} ions, J. Hazard. Mater. 289 (2015) 91–100.
[25] Z. Wang, Y. Feng, X. Hao, W. Huang, G. Guan, A. Abudula, An intelligent displacement pumping film system: A new concept for enhancing heavy metal ion removal efficiency from liquid waste, J. Hazard. Mater. 274 (2014) 436–442.
[26] N. Wang, J. Feng, J. Chen, J. Wang, W. Yan, Adsorption mechanism of phosphate by polyaniline/TiO_2 composite from wastewater, Chem. Eng. J. 316 (2017) 33–40.
[27] J. Yu, X. Zhao, J. Du, W. Chen, Preparation, microstructure and photocatalytic activity of the porous TiO_2 anatase coating by sol-gel processing, J. Sol-gel Sci. Techn. 17 (2000) 163–171.
[28] K.F. Schoch, W.A. Byers, L.J. Buckley, Deposition and characterization of conducting polymer thin films on insulating substrates, Synthetic Met. 72 (1995) 13–23.
[29] C.O. Yoon, M. Reghu, D. Moses, A.J. Heeger, Y. Cao, Electrical transport in conductive blends of polyaniline in poly(methyl methacrylate), Synthetic Met. 63 (1994) 47–52.
[30] M. Aldissi, S.P. Armes, X-ray photoelectron spectroscopy study of bulk and colloidal polyaniline, Macromolecules 25 (1992) 2963–2968.
[31] J.Y. Ha, T.P. Trainor, F. Farges, G.E. Brown, Interaction of Zn(II) with hematite nanoparticles and microparticles: part 2. ATR-FTIR and EXAFS study of the aqueous Zn(II)/oxalate/hematite ternary system, Langmuir 25 (2009) 5586–5593.
[32] M. Angelopoulos, G.E. Asturias, S.P. Ermer, A. Ray, E.M. Scherr, A.G. Macdiarmid, M. Akhtar, Z. Kiss, A.J. Epstein, Polyaniline: solutions, films and oxidation state, Mol. Crys. Liq. Cryst. Inc. Nonlinear Opt. 160 (1988) 151–163.
[33] Y. Zhu, Z. Li, G. Chong, L. Cao, The synthesis of nanosized TiO_2 powder using a sol-gel method with TiCl4 as a precursor, J. Mater. Sci. 35 (2000) 4049–4054.
[34] F.A. Rafiqi, K. Majid, Comparative effect of chelated and non-chelated metal complexes of Ni(II), Zn(II), Tb(III), Fe(II) and Fe(III) on the thermal stability of polyaniline composites, J. Therm. Anal. Calorim. 130 (2017) 1759–1767.
[35] J.C. Yu, J.G. Yu, W.K. Ho, Z.T. Jiang, L.Z. Zhang, Effects of F^- doping on the photocatalytic activity and microstructures of nanocrystalline TiO_2 powders, Chem. Mater. 14 (2002) 3808–3816.
[36] J. Chen, J. Feng, W. Yan, Influence of metal oxides on the adsorption characteristics of PPy/metal oxides for methylene blue, J. Colloid. Interf. Sci. 475 (2016) 26–35.
[37] J. Chen, C. Shu, N. Wang, J. Feng, H. Ma, W. Yan, Adsorbent synthesis of polypyrrole/TiO_2 for effective fluoride removal from aqueous solution for drinking water purification: adsorbent characterization and adsorption mechanism, J. Colloid. Interf. Sci. 495 (2017) 44–52.
[38] I. Langmuir, The adsorption of gases on plane surfaces of glass, mica and platinum, J. Am. Chem. Soc. 40 (1918) 1361–1403.
[39] H. Freundlich, Concerning adsorption in solutions, Zeitschrift Fur Physikalische Chemie-Stochiometrie Und Verwandtschaftslehre 57 (1906) 385–470.
[40] M.M. Dubinin, E.D. Zaverina, V.V. Serpinsky, The sorption of water vapour by active carbon, J. Chem. Soc. 60 (1955) 1760–1766.
[41] M. Temkin, V. Pyzhev, Kinetics of ammonia synthesis on promoted iron catalysts, Acta Physicochim. URSS 12 (1940) 327–356.
[42] N. Moazezi, M. Baghdadi, M.A. Hickner, M.A. Moosavian, Modeling and experimental evaluation of Ni(II) and Pb(II) sorption from aqueous solutions using a Polyaniline/$CoFeC_6N_6$ nanocomposite, J. Chem. Eng. Data 63 (2018) 741–750.
[43] M.A. Moosavian, N. Moazezi, Removal of cadmium and zinc ions from industrial wastewater using nanocomposites of PANI/ZnO and PANI/CoHCF: a comparative study, Desalin. Water Treat. 57 (2016) 20817–20836.
[44] M. Omraei, H. Esfandian, R. Katal, M. Ghorbani, Study of the removal of Zn(II) from aqueous solution using polypyrrole nanocomposite, Desalination 271 (2011) 248–256.
[45] Y. Liu, L. Chen, Y. Li, P. Wang, Y. Dong, Synthesis of magnetic polyaniline/graphene oxide composites and their application in the efficient removal of Cu(II) from aqueous solutions, J. Environ. Chem. Eng. 4 (2016) 825–834.
[46] M. Visa, A. Duta, TiO_2/fly ash novel substrate for simultaneous removal of heavy metals and surfactants, Chem. Eng. J. 223 (2013) 860–868.
[47] Z. Ping, B. Gerhard, E. Nauer, H. Neugebauer, J. Theiner, A. Neckel, Protonation and electrochemical redox doping processes of polyaniline in aqueous solutions: investigations using in situ FTIR-ATR spectroscopy and a new doping system, J. Chem. Soc. Faraday Trans. 93 (1997) 121–129.
[48] E.T. Kang, K.G. Neoh, K.L. Tan, Protonation and deprotonation of polyaniline films and powders revisited, Synthetic Met. 68 (1995) 141–144.